

Validation of GOES-Based Insolation Estimates Using Data from the U.S. Climate Reference Network

JASON A. OTKIN AND MARTHA C. ANDERSON

Space Science and Engineering Center, Cooperative Institute for Meteorological Satellite Studies, University of Wisconsin—Madison, Madison, Wisconsin

JOHN R. MECIKALSKI

Department of Atmospheric Sciences, University of Alabama in Huntsville, Huntsville, Alabama

GEORGE R. DIAK

Space Science and Engineering Center, Cooperative Institute for Meteorological Satellite Studies, University of Wisconsin—Madison, Madison, Wisconsin

(Manuscript received 19 July 2004, in final form 2 March 2005)

ABSTRACT

Reliable procedures that accurately map surface insolation over large domains at high spatial and temporal resolution are a great benefit for making the predictions of potential and actual evapotranspiration that are required by a variety of hydrological and agricultural applications. Here, estimates of hourly and daily integrated insolation at 20-km resolution, based on Geostationary Operational Environmental Satellite (GOES) visible imagery are compared to pyranometer measurements made at 11 sites in the U.S. Climate Reference Network (USCRN) over a continuous 15-month period. Such a comprehensive survey is necessary in order to examine the accuracy of the satellite insolation estimates over a diverse range of seasons and land surface types. The relatively simple physical model of insolation that is tested here yields good results, with seasonally averaged model errors of 62 (19%) and 15 (10%) W m^{-2} for hourly and daily-averaged insolation, respectively, including both clear- and cloudy-sky conditions. This level of accuracy is comparable, or superior, to results that have been obtained with more complex models of atmospheric radiative transfer. Model performance can be improved in the future by addressing a small elevation-related bias in the physical model, which is likely the result of inaccurate model precipitable water inputs or cloud-height assessments.

1. Introduction

Detailed knowledge of the spatial and temporal distribution of incoming solar radiation (insolation) at the earth's surface has the potential utility for a wide range of hydrologic and agronomic applications, including estimation of regional evapotranspiration and carbon fluxes, management of water supply, and implementation of precision agricultural practices. During the last several decades, satellite data have been used to esti-

mate insolation from hourly to monthly time scales. Geostationary satellites, such as the Geostationary Operational Environmental Satellite (GOES), have a distinct advantage over ground-based pyranometer networks and polar-orbiting platforms in their ability to provide continental-scale insolation data with high spatial (≥ 1 km) and temporal (≥ 15 min) resolution. Such finely resolved insolation maps provide an excellent opportunity to study climate and the surface energy budget.

Both statistical and physical methods have been created to estimate surface insolation from satellite data. Tarpley (1979) developed a statistical method that empirically related satellite-measured brightness and cloud amount to hourly pyranometer insolation measurements, yielding reasonable results. Statistical meth-

Corresponding author address: Jason A. Otkin, Cooperative Institute for Meteorological Satellite Studies, Space Science and Engineering Center, University of Wisconsin—Madison, 1225 W. Dayton Street, Madison, WI 53706.
E-mail: jasono@ssec.wisc.edu

ods, however, are inappropriate for global implementation, because the data must be “tuned” to a given pyranometer location. Physically based methods explicitly simulate reflection, scattering, and absorption processes that are active in the earth–atmosphere column at varying levels of complexity, and are more generally applicable over large geographical regions. A simple physical method using first-generation GOES visible data was developed by Gautier et al. (1980), with improvements made thereupon by Diak and Gautier (1983). Subsequent work by Gautier et al. (1984), Möser and Raschke (1984), Pinker and Ewing (1985), Dedieu et al. (1987), Darnell et al. (1988), Frouin and Chertock (1992), Pinker and Laszlo (1992), and Weymouth and Le Marshall (1999) have either improved the detail of the various physical methods or extended their application to other geostationary satellites.

Detailed reviews by Schmetz (1989) and Pinker et al. (1995) highlight the ability of remote sensing methods to produce reasonably accurate insolation estimates over a wide range of temporal scales. Their comprehensive surveys revealed that daily insolation estimates are generally within 10%–15% of pyranometer data, while hourly estimates have errors that range from 5%–10% for clear-sky conditions to 15%–30% for all-sky conditions. More recent studies employing data from several different geostationary satellites continue to corroborate the accuracy of these earlier insolation studies. For instance, Stewart et al. (1999) and Garatuza-Payan et al. (2001) report hourly errors of 14% and 20%, respectively, over the Yaqui Valley of northwestern Mexico, while Kawamura et al. (1998) obtained agreement to within 17% of hourly measurements over the western Pacific.

In this study, hourly and daily integrated GOES-based insolation estimates that are produced at the University of Wisconsin—Madison at 20-km resolution will be compared to pyranometer data from 11 sites in the U.S. Climate Reference Network (USCRN) over a continuous 15-month period. The satellite estimates were created using the method of Gautier et al. (1980) and Diak and Gautier (1983), which embody a relatively simple physical representation of cloud and atmospheric radiative transfer processes. This simple model is found to perform as well as more complex parameterizations over a diverse range of seasons, climatic conditions, and land surface types, and has been implemented operationally to generate near-real-time insolation fields for regional- and continental-scale land surface carbon and water flux assessments (Mecikalski et al. 1999; Anderson et al. 2003; Anderson et al. 2004), subsurface hydrologic modeling efforts, and agricul-

tural forecasting products (Diak et al. 1998; Anderson et al. 2001). (Hourly and daily integrated insolation estimates are available on a next-day basis. Daily-integrated insolation is available online at <http://www.soils.wisc.edu/wimnext/sun.html>. Hourly data over the continental United States back to 2002 can be obtained by request from the authors.)

Section 2 describes the physical model that is used to estimate surface insolation from GOES satellite data, while section 3 discusses satellite imagery and USCRN data collection and processing techniques. Validation results for the hourly- and daily- integrated satellite-estimated insolation data are presented in section 4. Limitations and future improvements to the physical model are discussed in section 5, with conclusions in section 6.

2. Model description

The radiative transfer model that is employed in this study to estimate surface insolation from GOES visible imagery is described in detail by Gautier et al. (1980), with improvements made thereupon by Diak and Gautier (1983) (hereafter referred to as the GDM model). The physical model is based on the conservation of radiant energy within the earth–atmosphere column and contains separate parameterizations for cloudy and clear-sky conditions (Fig. 1). These parameterizations are relatively simple, for example, in comparison with the physical model of Pinker and Laszlo (1992) that was adopted by the Global Energy and Water Cycle Experiment (GEWEX) program, which incorporates detailed transmission models in five spectral bands within the solar spectrum and a more explicit treatment of cloud microphysical processes. The GDM model is more “bulk” in nature and is a de facto two-band approach, considering only radiative transfer processes within the water vapor absorption region between approximately 0.4 and 0.7 μm , and transfer outside of this region.

In the GDM approach, a decision to apply a clear- or cloudy-sky atmospheric parameterization is made on an hourly basis by comparing instantaneous visible images of calibrated top-of-atmosphere reflectance with a reference clear-sky map of the surface albedo. The “clear sky” albedo map is constructed as a composite of the minimum surface albedo that is computed at each grid cell over the prior 2-week period, using the GOES visible image that is closest to solar noon in order to minimize variability resulting from the view angle. Regular (at least biweekly) updating of the albedo field is necessary in order to capture seasonal changes in vegetation, soil moisture, and snow cover.

GOES Insolation Model

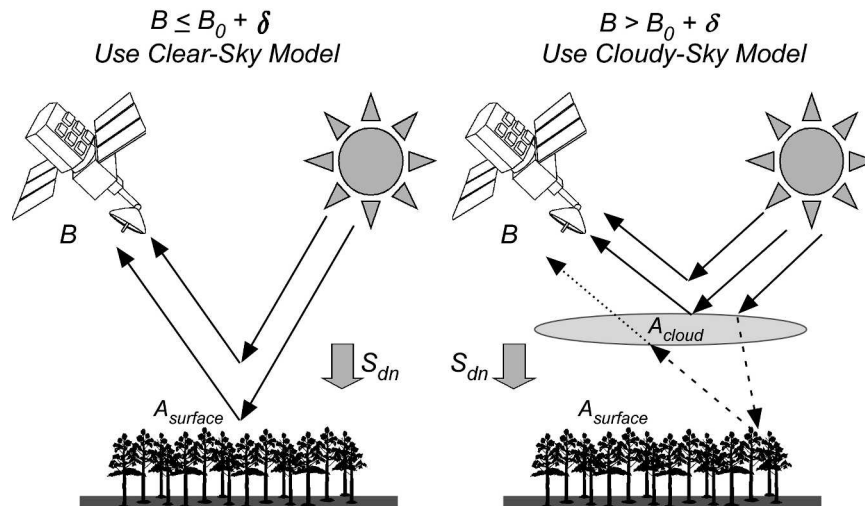


FIG. 1. Graphical depiction of the physical model employed for (left-hand side) clear-sky conditions and (right-hand side) cloudy-sky conditions; B refers to the brightness observed by the satellite, while B_0 is the clear-air brightness threshold modified by a small confidence margin δ to account for errors in albedo and atmospheric water vapor and aerosol concentrations; S_{dn} refers to the downward shortwave radiation flux; and $A_{surface}$ and A_{cloud} refer to the surface and cloud albedos, respectively.

The clear-sky albedo is then used along with atmospheric ozone, water vapor, and sun angle information to estimate the digital brightness that the satellite would measure under clear-sky conditions at a given location in the model domain. If the actual brightness of the instantaneous data point is at or below the clear-sky threshold, a clear-sky model of the atmosphere that accounts for Rayleigh scattering, water vapor absorption, and ozone absorption is employed to estimate the surface insolation. If the measured brightness exceeds the clear-sky threshold, a cloudy model is used to calculate the surface insolation. With the cloudy model, a cloud albedo is computed from the GOES visible imagery, taking into account atmospheric effects above the cloud top. Then, a simple parameterization that accounts for Rayleigh scattering, ozone absorption, and water vapor absorption above and below the cloud is used to predict insolation at the land surface. The cloudy model assumes plane-parallel clouds and is optimized for low- and midlevel clouds because these clouds most strongly influence the magnitude of the surface insolation.

In the GDM model, ozone absorption is estimated following the method of Lacis and Hansen (1974), which treats the ozone layer as an absorbing medium overlying a reflecting surface layer. With this method, empirical formulas are used to estimate ozone absorp-

tion in the ultraviolet range and in the GOES visible channel, which together describe the effect of ozone absorption on the total solar flux at the surface. The broadband absorption of solar flux by water vapor is modeled following the method of Paltridge (1973). The total column water vapor that is used by this method is obtained from the precipitable water field in the 1200 UTC initialization of the Cooperative Institute for Meteorological Satellite Studies (CIMSS) Regional Assimilation System (CRAS) model (Diak et al. 1992), which is initialized with the National Centers for Environmental Prediction (NCEP) Eta model fields. The current version of the radiative transfer model does not include a parameterization for the scattering and absorption of solar radiation by atmospheric aerosols. Although aerosols can strongly effect the surface insolation, the highly variable and poorly known distribution of atmospheric aerosols impedes an accurate representation of the complex interaction between aerosols and radiation.

Previous validation experiments with the GDM model have suggested an accuracy rivaling that of more complex parameterizations, but, to date, have been conducted only over a limited range of land surface and climatic conditions. Gautier et al. (1984) and Diak et al. (1996) found errors in daily-integrated insolation of 9%–10% of the observed mean in comparison with

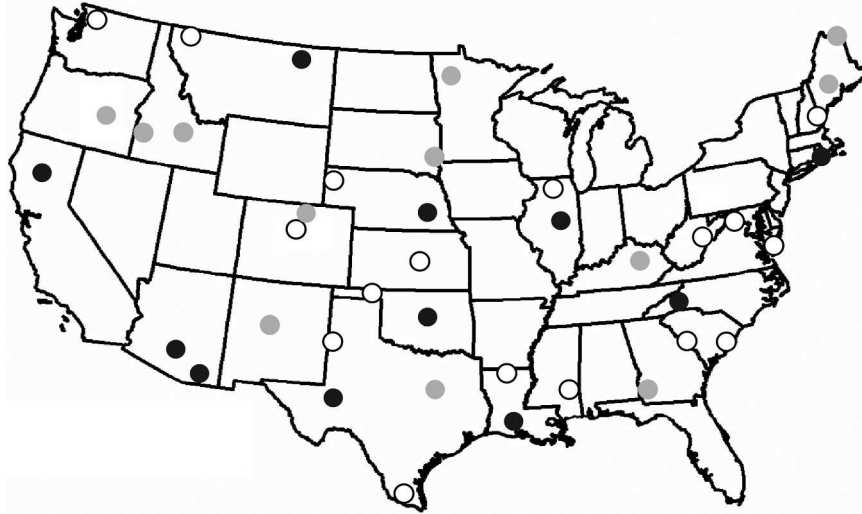


FIG. 2. USCRN locations across the continental United States as of early 2004. Stations indicated by black circles were used for the seasonal satellite-derived insolation comparison (section 4). Stations indicated by either black or gray circles were used to evaluate an elevation-related bias in the physical model (section 5). Stations indicated by clear circles were not used in this study.

pyranometer data collected in southern Canada and Wisconsin. Similar accuracies were reported by Frouin et al. (1988) in comparison with shipborne measurements off of the California coast. Raphael and Hay (1984) obtained 17% and 9% agreement with hourly and daily measurements, respectively, from a 12-station pyranometer network in British Columbia. Jacobs et al. (2002) reported hourly and daily errors of 28% and 10%, respectively, for very complex summer cloud conditions over northern Florida.

3. Data processing and analysis

a. GOES-derived insolation fields

For this study, data from three GOES satellites were used to map surface insolation on a 0.2° latitude \times 0.2° longitude grid (~ 20 km resolution) across the continental United States. Hourly insolation over the western United States (west of 100°W) was calculated at the top of each hour using data from the *GOES-10* satellite (hereafter referred to as GOES-W). Prior to 14 May 2003, hourly insolation for the eastern United States was obtained from *GOES-8* satellite data at 15 min past the top of the hour. After this date, insolation was calculated using *GOES-12* satellite data. The *GOES-8* and *-12* satellites will collectively be referred to as GOES-E.

While the GOES visible instruments have a nadir spatial resolution of 1 km, the insolation algorithm is applied to data that have been prior averaged to 2-km

resolution to reduce effects of navigational “jitter” that is evident in the raw imagery. Insolation estimates are then averaged over 10×10 pixel boxes to fill the 20-km grid.

b. USCRN insolation data

The USCRN is a nationwide network that is currently being developed to provide continuous, high-quality data of key climate-related variables, such as near-surface air temperature, precipitation, solar radiation, wind speed, and ground surface temperature. As of early 2004, the network consisted of approximately 40 stations across the continental United States (Fig. 2), and will contain 300 stations nationwide when fully implemented (National Climatic Data Center 2003).

Of particular interest for the present study is the availability of high-quality surface insolation measurements made by the USCRN. Insolation is measured at each site using a Kipp and Zonen SP Lite photodiode pyranometer, which is characterized by a spectral response in the $0.4\text{--}1.1\text{-}\mu\text{m}$ spectral range. Insolation measurements are taken every 2 s and then averaged to obtain 5-min insolation values. A station’s data stream at the top of each hour contains the average and standard deviation of the 12 five-minute insolation values during the previous hour.

Because of the short history of the USCRN (the first station came online in late 2001), insolation data were available from only a small number of stations at the

TABLE 1. The operational date, latitude, longitude, elevation (m), and land cover type for each of the 11 USCRN stations used for the insolation comparison. The satellite-derived insolation data that each station is compared to is shown in the last column

Station	Date	Lat (°)	Lon (°)	Elevation (m)	Land cover	GOES
Redding, CA	25 Mar 2003	40.65	122.61	445	Forest	West
Tucson, AZ	17 Sep 2002	32.24	111.17	844	Desert	West
Elgin, AZ	16 Sep 2002	31.59	110.51	1481	Arid grassland	West
Wolf Point, MT	20 Dec 2001	48.31	105.10	634	Semiarid grass	West
Monahans, TX	21 May 2003	31.62	102.81	852	Semiarid grass	West
Stillwater, OK	18 Mar 2002	40.69	97.10	277	Forest	East
Lincoln, NE	14 Jan 2002	36.12	96.85	416	Agricultural	East
Lafayette, LA	11 Jan 2003	30.09	91.87	11	Forest	East
Champaign, IL	22 Dec 2002	40.05	88.37	210	Agricultural	East
Asheville, NC	1 Aug 2001	35.42	82.56	640	Forest	East
Kingston, RI	16 Dec 2001	41.49	71.54	43	Forest	East

beginning of this study (1 December 2002). Therefore, in order to attain a relatively even distribution of stations across the United States, insolation data from several USCRN stations that were implemented after December 2002 have also been utilized (Table 1). The USCRN sites chosen for this study encompass a wide distribution of land surface types, ranging from heavily forested land (Asheville, North Carolina) to flat agricultural land (Champaign, Illinois), complex coastal areas (Lafayette, Louisiana), semiarid grasslands (Wolf Point, Montana), and desert regions (Tucson, Arizona).

c. Hourly and daily insolation data streams

In the following sections, hourly and daily integrated insolation data from 11 sites in the USCRN (Fig. 2) are compared to GOES insolation estimates extracted from the grid point that is nearest to the site over a continuous 15-month period from 1 December 2002 to 29 February 2004. To identify any seasonal variations in the accuracy of the satellite estimates, the 15-month period has been divided into five standard meteorological seasons (i.e., spring occurs from March to May; summer occurs from June to August, etc.).

To better synchronize the modeled and measured data streams, the time stamps that are associated with the USCRN data points were shifted to represent the midpoint of the hourly averaging interval. Hourly GOES-based insolation estimates were then linearly interpolated to these time stamps. Both modeled and measured hourly time series were accumulated using trapezoidal integration to represent the daily total insolation.

Gaps in the satellite image record (resulting from power outages and hardware problems) have been filled by linear interpolation if the gaps did not exceed 1 h in length. No attempt was made to remove gaps

consisting of two or more consecutive hours of missing insolation data; on these days, the daily-integrated satellite-estimated insolation was not calculated. Gap filling was not performed on the hourly USCRN insolation dataset and the daily-integrated insolation was not calculated for a given day if any hourly USCRN insolation measurements were missing.

No additional screening was applied to either dataset, except to remove nighttime values of zero insolation (which artificially inflate model accuracy estimates) and days on which a site had measurable snow cover. The insolation algorithm in its current form is unable to distinguish between snow cover and clouds, leading to severe underestimation of insolation (see section 5c); this is a limitation common to most insolation models based on visible satellite imagery. Snow-covered days were identified at each station by examining hourly temperature and precipitation records.

d. Uncertainties in pyranometer–satellite comparisons

Both modeled and measured insolation data streams contain instrumental errors. In addition, uncertainties in comparison also arise because of fundamental differences that are inherent in the mode and scale of measurements obtained by ground-based pyranometers and geostationary satellites.

While the SP Lite photodiode sensor that is employed by the USCRN is a reliable instrument that can be used during all weather conditions, several minor instrument-related errors can occur. These errors include directional or cosine response errors, a slightly nonlinear instrument response function, and issues that are associated with long-term instrument stability. The cosine response error, which refers to the accuracy of the sensor for different sun angles, is <1% for angles of

incidence $<60^\circ$ and increases to $\pm 5\%$ for a sun angle of 80° . The instrument response function, which calculates the insolation from the magnitude of the voltage that is measured by the sensor, has a minor nonlinearity of $<1\%$ for insolation up to 1000 W m^{-2} . Finally, although errors associated with long-term sensor degradation are expected to be relatively small (sensor stability is $< \pm 2\% \text{ yr}^{-1}$), sensor recalibration is still necessary every 1–2 yr. In this study, no attempts were made to account for long-term drifts in the insolation measurements or for “jumps” when sensors were recalibrated or exchanged. Typically, expected accuracy on the order of 5% is quoted for pyranometer data.

Apart from any problems in the physical model, satellite sensor degradation and errors in image navigation can also impact the accuracy of the GOES insolation data. Although image navigation errors may be very important for individual pixels, it is suspected that the magnitude of this error should decrease at the relatively coarse resolution that is used for this study. While the visible imagers on the GOES satellites are not calibrated in orbit, substantial long-term degradation was not evident during the course of this study; therefore, no attempt was made to account for sensor drift.

Perhaps more important than these instrumental effects in terms of influencing scatter in model–measurement comparisons are issues of temporal and spatial scale. Given the steep rise in the clear-sky diurnal insolation curve, small mismatches in timing can induce significant scatter. Furthermore, pyranometer data are typically reported as time averages, whereas a satellite provides an instantaneous snapshot of horizontally averaged surface conditions. Effects of unresolved clouds at the 20-km scale will be evident at the hourly scale, but will tend to average out over longer intervals. Finally, while ground-based pyranometers sample an upward-looking hemispherical solid angle, a satellite image pixel collects flux from a much smaller solid angle view. Some of this mismatch in volume sampling may be addressed in the 10×10 pixel averaging that has been applied to the gridded insolation fields (Gautier et al. 1984).

4. Results

Seasonal comparisons of hourly and daily insolation measurements from 11 USCRN stations across the continental United States, with estimates derived from GOES-E and GOES-W imagery, are presented in Figs. 3 and 4. Statistical measures that are used to describe these comparisons include the coefficient of determination (R^2), the mean bias error (MBE), and the root-mean-square difference (rmsd) between the modeled

and observed data (also expressed as a percentage of the mean observed value). Statistics that are averaged over all seasons for stations in the east and west domains, and for all stations combined, are shown in Table 2.

For the GOES-E hourly comparisons (Fig. 3a), the highest seasonal correlations ($R^2 = 0.94\text{--}0.96$) generally occurred within relatively flat agricultural regions that are characterized by a continental climate (i.e., Lincoln, Nebraska, Stillwater, Oklahoma, and Champaign, Illinois). Coastal areas (Kingston, Rhode Island, and Lafayette, Louisiana) and mountainous regions (Asheville, North Carolina) tended to have the lowest correlations each season. The accuracy of the hourly GOES-E insolation data for all seasons and stations was comparable to previous studies (which were generally of a more limited scope), with an average rmsd of 62 W m^{-2} (20% of the mean observed value). Given the complex cumulus cloud environment characteristic of warmer seasons, it is not surprising that the largest average seasonal rmsd ($\sim 23\%$) and the lowest average seasonal correlation ($R^2 = 0.90$) occurred during the summer.

Considering the complex topography that surrounds many of the western USCRN stations, the average rmsd was notably low, at 66 W m^{-2} (18%; see Fig. 3b). The relative magnitude of the rmsd was closely tied to the local climate conditions. For instance, the satellite-estimated insolation data at Redding, California, attained a relatively small rmsd (11%–14%) during the benign weather characteristic of the summer and fall seasons, and then had a much larger rmsd (28%) during the winter season, which is characterized by the passage of numerous cyclones across the region. Likewise, the rmsd at the two Arizona stations was largest during the summer (rmsd of 15%–25%) when the North American monsoon (Tang and Reiter 1984; Higgins et al. 1997) was active, and also during the winter (rmsd of 18%–21%), when the region was influenced by extratropical cyclones.

Figure 4a contains seasonal comparisons of daily-integrated USCRN and GOES-E insolation data. Temporal averaging has reduced the scatter considerably, yielding high linear correlations ($R^2 > 0.96$) and low rmsd ($<10\%$). The average rmsd of $1.3 \text{ MJ m}^{-2} \text{ day}^{-1}$ (15 W m^{-2} ; 10% of the mean observed value) over all eastern stations and seasons compares favorably to previous satellite-derived insolation studies. The relative rmsd was lowest during the fall of 2003 (8%) and highest during the winter of 2002/03 (12%).

Daily-integrated GOES-W and USCRN insolation data are compared in Fig. 4b. The average rmsd for all western stations and seasons is $1.4 \text{ MJ m}^{-2} \text{ day}^{-1}$ (16 W m^{-2} ; 9% of the mean observed value), which is slightly

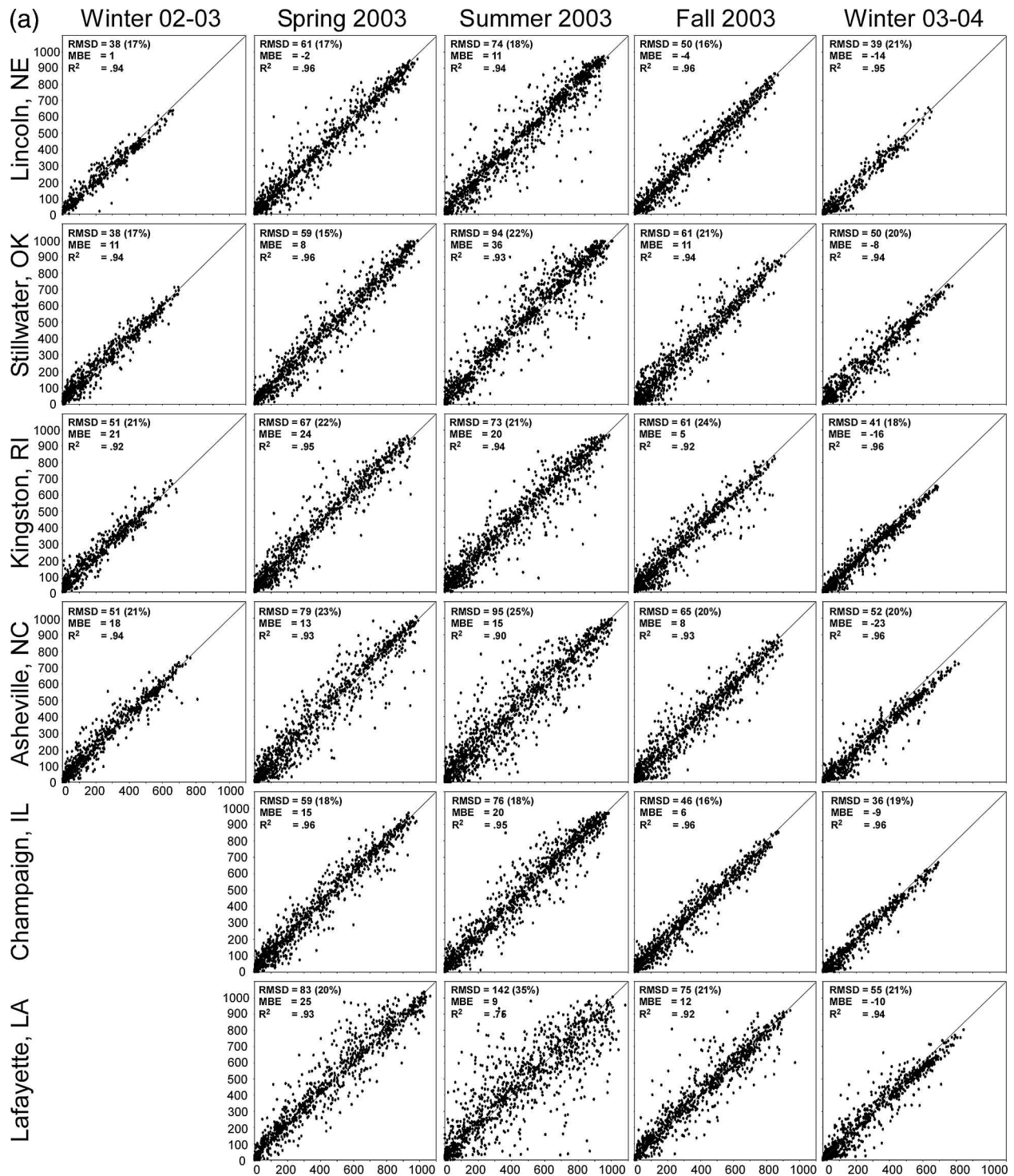


FIG. 3. Seasonal comparison of hourly insolation (W m^{-2}) estimated from (a) GOES-E and (b) GOES-W imagery (plotted along the ordinate of each panel) and data from 11 USCRN stations (plotted along the abscissa of each panel). Station names are indicated along the left-hand side of the figure; seasons are indicated at the top. Rmsd as a percent of the mean observed flux is indicated in parentheses.

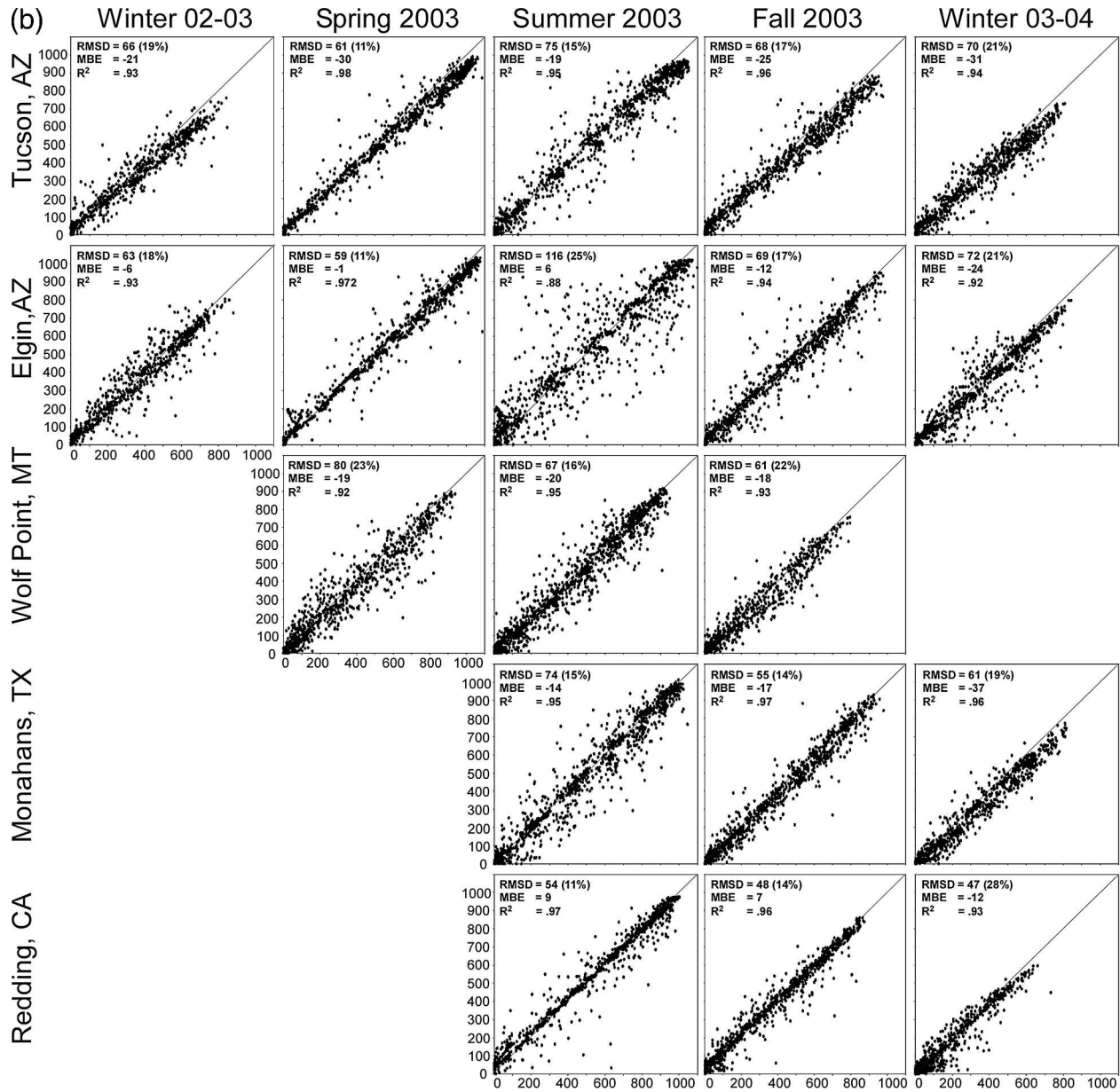


FIG. 3. (Continued)

better than the daily-integrated GOES-E insolation results. Together, the GOES-E and GOES-W results illustrate the ability of the simple physical GDM model to accurately estimate the surface insolation over a diverse set of seasons and locations.

5. Discussion

a. Systematic biases in estimated insolation

While overall correlations between modeled and measured insolation are reasonable at the hourly and

daily time scale, the statistical comparisons that are discussed in section 4 reveal systematic biases related to season, satellite platform, and local site characteristics. Figure 5 compares monthly averaged rmsd, MBE, and R^2 that are associated with stations within the GOES-E and GOES-W imaging domains, as evaluated from both the hourly and daily data streams, with average statistics over all of the seasons given in Table 2. It is evident that the GOES-W insolation estimates exhibit slightly higher rmsd and bias magnitude than GOES-E. For all stations combined (east and west), the average rmsd is 63 W m^{-2} for hourly data and 16 W m^{-2} for

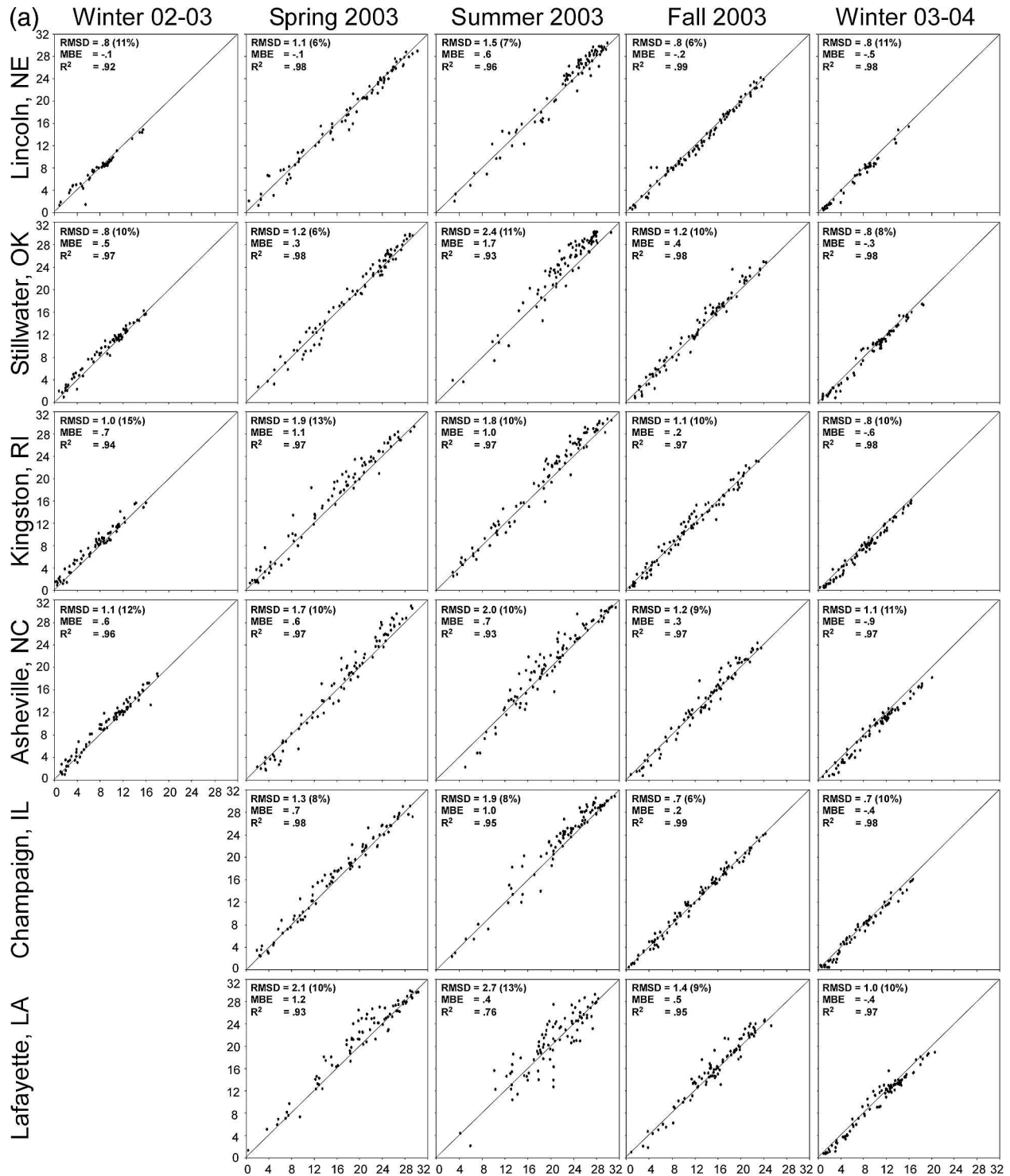


FIG. 4. Same as Fig. 3, except for daily insolation ($\text{MJ m}^{-2} \text{day}^{-1}$).

daily data. This can be compared to the results of Pinker et al. (2003), who obtained an rms agreement of 83–95 (hourly) and 21–25 (daily) W m^{-2} when days with snow cover were removed.

Seasonally, both satellites yield the largest rmsd and lowest R^2 during the summer months (Fig. 5), when cloud conditions are expected to be most variable. Seasonal trends in the MBE are also similar for each sat-

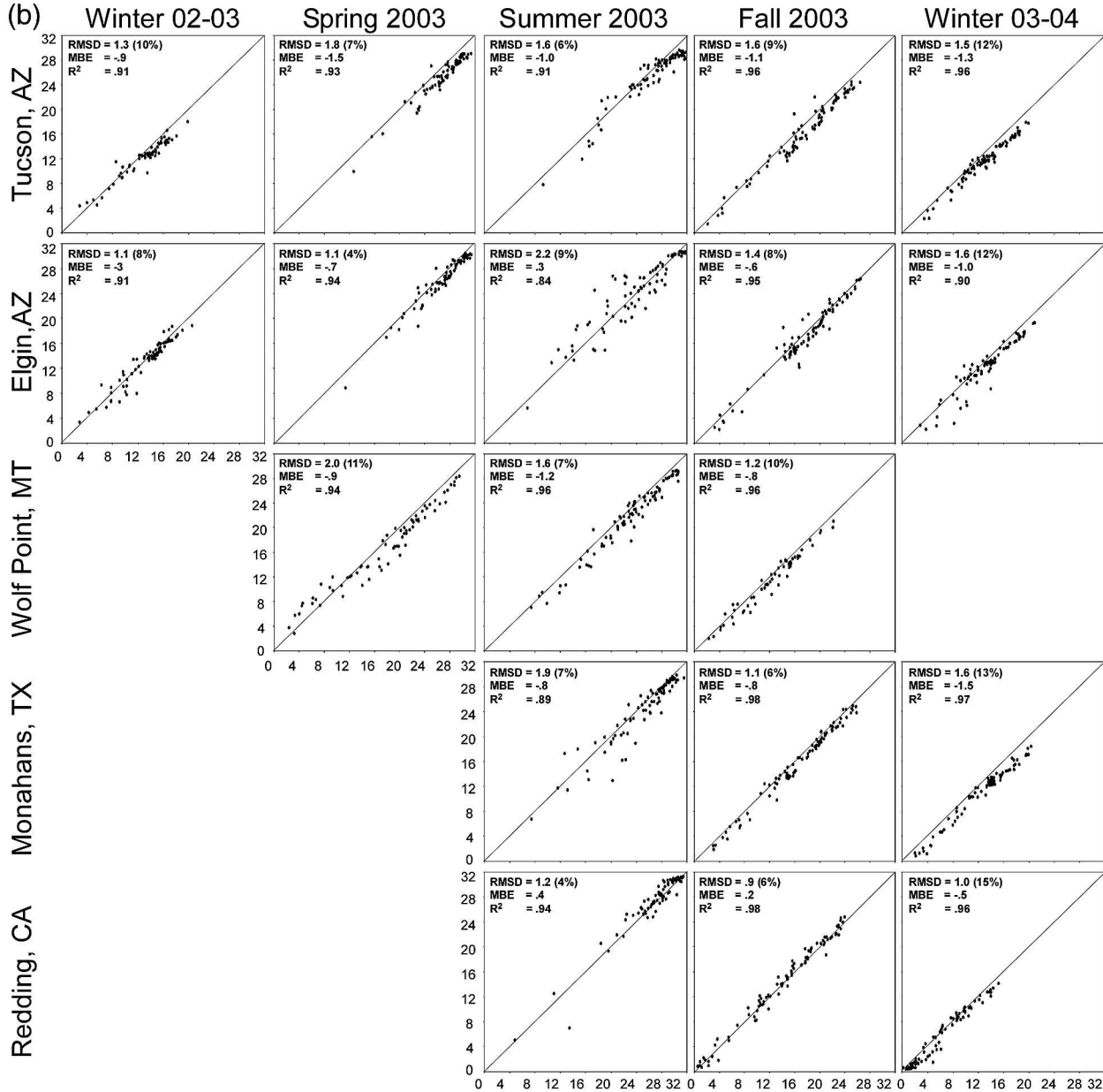


FIG. 4. (Continued)

ellite, with MBE generally being more positive during the summer months. Pinker et al. (2003) showed similar seasonal trends in bias in GOES-estimated insolation. The direction of the bias error, however, is markedly different for the two satellite platforms, with GOES-E tending to overestimate observed insolation by 8 and 4 $W m^{-2}$ for hourly and daily evaluations, respectively, and GOES-W yielding an underestimation of -17 (hourly) and -9 (daily) $W m^{-2}$, on average.

This GOES-E/-W-specific behavior may be related to differences between the satellite platforms (e.g., sen-

sor calibration, view angle with respect to the sun angle), but may also be attributable, in part, to site characteristics and biases that are inherent in the physical model. Of the USCRN stations that are considered in this study, sites in the western half of the United States tended to be at higher elevations (see Table 1). Mean bias errors that are computed for 23 USCRN stations (cf. Fig. 2) during the fall of 2003 (1 September 2003–30 November 2003) are plotted versus station elevation in Fig. 6. This time period was chosen in order to include a large sample of USCRN stations and yet

TABLE 2. Quantitative measures of model performance* in estimating insolation for USCRN stations in the GOES-W and -E domains, and for all stations combined, averaged over the five seasons shown in Figs. 3–4.

	Hourly			Daily		
	GOES-W	GOES-E	All	GOES-W	GOES-E	All
Rmsd W m^{-2} ($\text{MJ m}^{-2} \text{ day}^{-1}$)	65.9	61.6	63.3	16.6 (1.4)	14.8 (1.3)	15.5 (1.3)
MBE W m^{-2} ($\text{MJ m}^{-2} \text{ day}^{-1}$)	-16.6	7.8	-2.0	-8.9 (-0.8)	4.1 (0.4)	-1.1 (-0.1)
R^2	0.95	0.94	0.94	0.92	0.95	0.94

* Rmsd is the root-mean-square difference between the modeled (P) and observed (O) quantities; MBE is the mean-bias-error ($\bar{P} - \bar{O}$), where \bar{P} and \bar{O} are the mean modeled and observed fluxes, respectively; and R^2 is the coefficient of determination in a linear regression of P on O .

avoid the complex cloud conditions that prevailed during the summer and the presence of snow cover during the winter. This comparison suggests that the satellite-derived surface insolation is systematically overesti-

mated for stations at lower elevations (<300 m) and underestimated at higher elevation sites. This bias may be related to an overestimation in the physical model of precipitable water and/or water vapor at higher eleva-

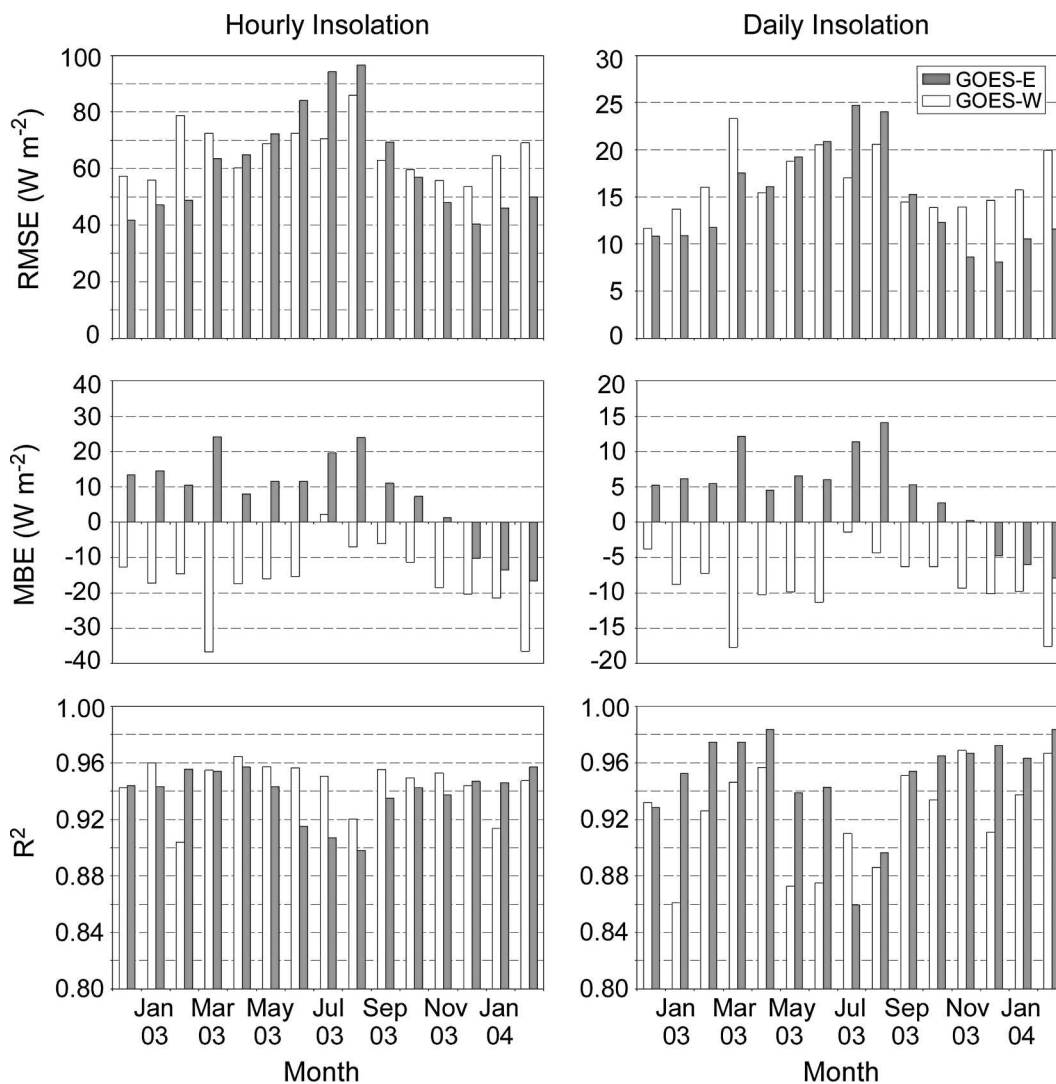


FIG. 5. (top) Monthly rmsd, (middle) MBE, and (bottom) R^2 for model-measurement comparisons in the GOES-E and GOES-W imaging domains at (left) hourly and (right) daily time scales.

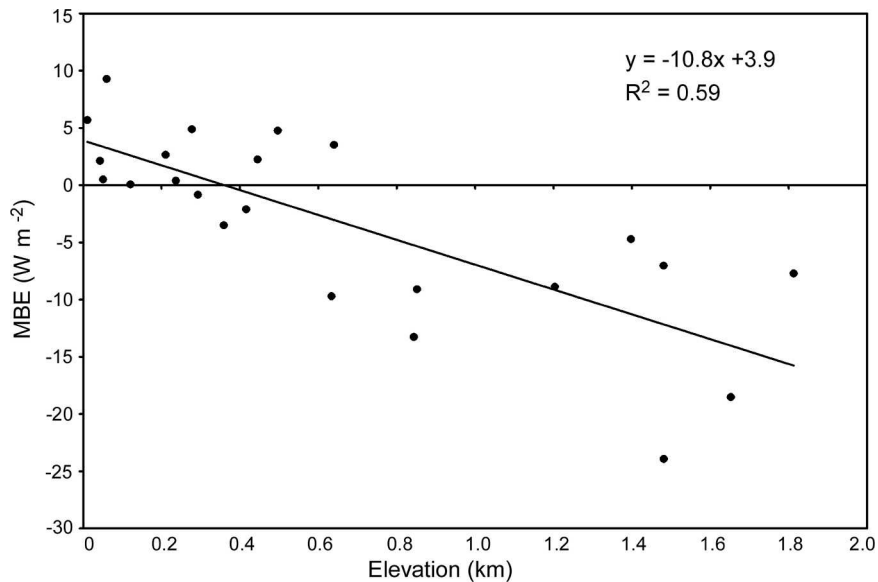


FIG. 6. Scatterplot of MBE for daily-integrated insolation estimates from 23 USCRN stations during the fall of 2003 (1 Sep 2003–30 Nov 2003) vs station elevation (km). The diagonal line describes the linear least squares regression, with regression coefficient and R^2 values as indicated.

tions, or to assumptions regarding cloud height relative to local surface topography. Further work will be needed to properly address this issue. The removal of this bias would further decrease the rmsd and MBE in model estimates from both satellites.

b. GOES-E/W overlap

USCRN stations in the overlap region ($\sim 95^\circ$ – 105° W longitude) between the GOES-E and -W operational imaging domains can be used to determine how well insolation estimates from these two satellite platforms agree over the study interval. Figure 7 compares a time series of hourly pyranometer data from Lincoln for the month of May 2003 with predictions from GOES-E and -W and an average of the two satellite estimates. In general, it is evident that the average value provides a better estimate of the measured insolation than does either satellite alone. Over the entire 15-month study interval, averaging the satellite data at Lincoln reduced the rmsd in the hourly comparison from 53–54 to 47 W m^{-2} , improved the R^2 from 0.95 to 0.97, and yielded MBEs midway between the biases that are exhibited by each satellite. A similar improvement was observed in the daily insolation data. It is often the case that one satellite will outperform the other in the morning, with the reverse case occurring during the afternoon; thus, the average gives the best estimate of the overall diurnal curve. This finding suggests that the eastern and western U.S. insolation fields are best stitched together

with a weighted average in the GOES-E/W overlap region, with weights for GOES-W, for example, increasing from 0 to 1 from longitudes 95° – 105° W. A representative spatial composite of insolation at 1800 UTC 20 May 2004, covering the continental United States, is shown in Fig. 8.

c. Snow cover effects

Most insolation models that are based on visible satellite imagery perform poorly over snow-covered regions because of an inability to distinguish between snow cover and clouds—both of which have high albedos in the visible band. As discussed earlier, the GDM model that was employed in this study uses the lowest surface albedo during the previous 2-week period as its background clear-sky surface albedo. If the preceding 2-week period was characterized by persistent snow cover, the background clear-sky albedo will be too high, and downwelling solar radiation at the land surface will be underestimated.

Figure 9 clearly illustrates this snow cover effect, where extensive snow cover across the northern United States (Fig. 9b) resulted in a background albedo that is more representative of cloudy conditions (Fig. 9a). The agricultural lands extending from western Iowa northwestward into southern Canada are especially susceptible to this problem as a result of their lower winter vegetation amount and more uniform snow cover, while adjacent snow-covered forested regions, such as

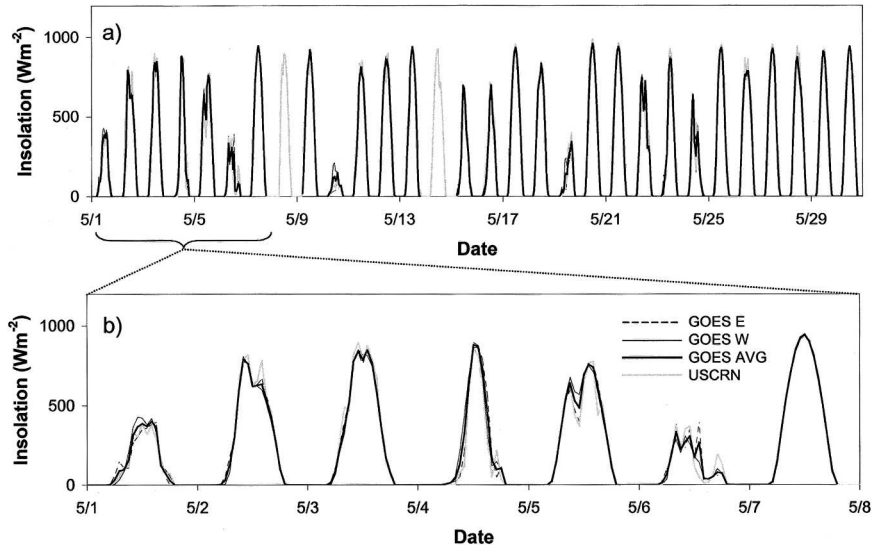


FIG. 7. Hourly time series of modeled and measured insolation at Lincoln, NE, for (a) the month of May 2003 and (b) an enlarged look at a sequence of days 1–7 May. Lines indicate estimates from GOES-E (thin dotted) and -W (thin solid) imagery, the GOES-E/W model average (thick black), and measurements from the Lincoln USCRN station (thick gray).

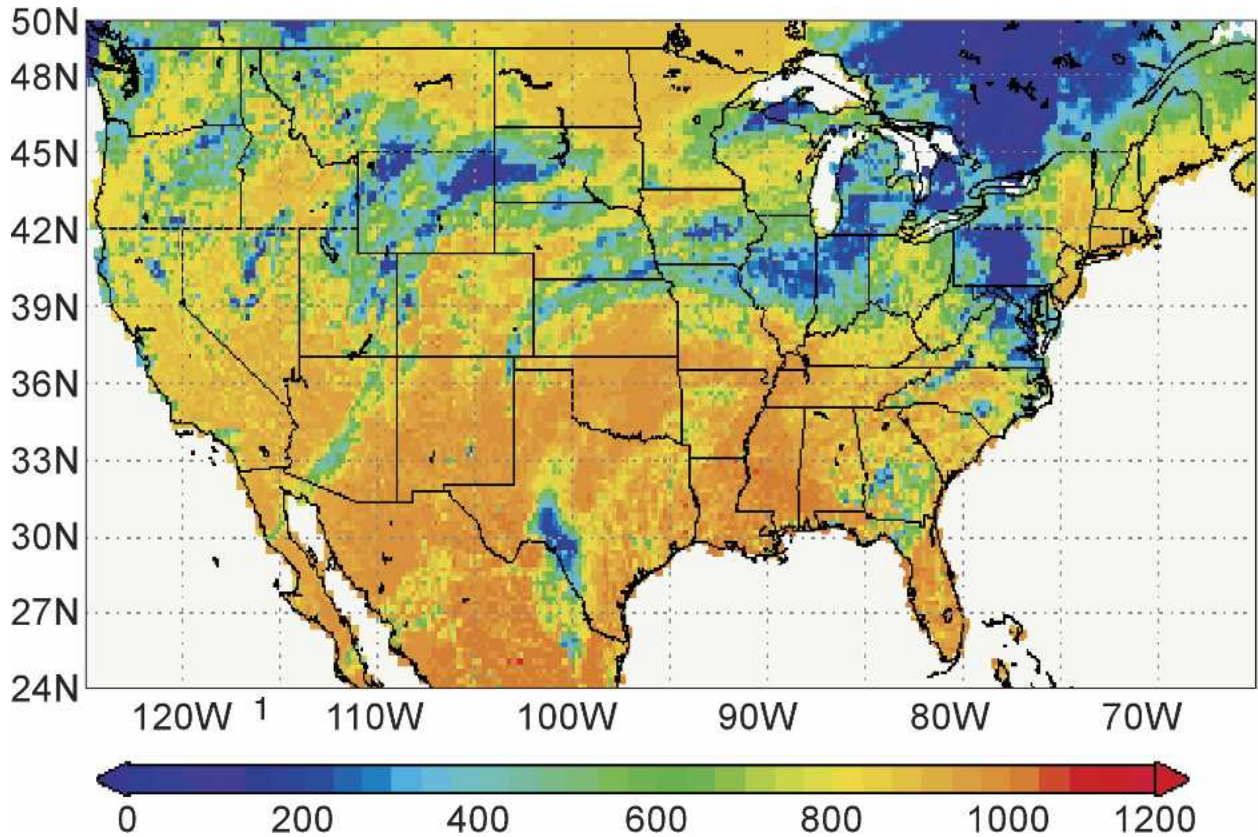


FIG. 8. Instantaneous insolation ($W m^{-2}$) across the continental United States generated from GOES-E and GOES-W satellite imagery for 1800 UTC 20 May 2004.

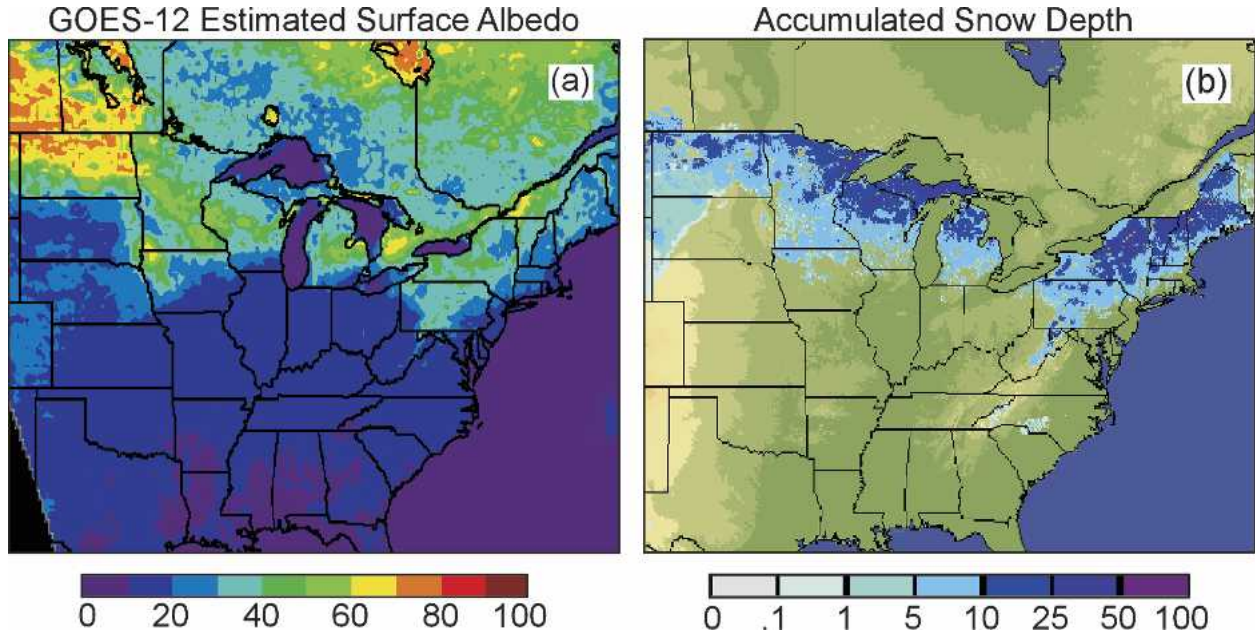


FIG. 9. (a) Reference surface albedo (%) estimated for 29 Feb 2004. (b) Accumulated snow depth (cm) across the eastern United States for 29 Feb 2004. (Snow depth data are courtesy of the National Operational Hydrologic Remote Sensing Center and are based on measurements collected within the United States, thus values indicated for southern Canada may not be accurate.)

those in northern Minnesota and Wisconsin, have a relatively low albedo for the same amount of snow.

The adverse effect of snow cover on insolation estimates can also be observed in the time series of daily

integrated insolation for Sioux Falls, South Dakota, shown in Fig. 10. For instance, the presence of extensive snow cover across the Northern Plains from 25 January to 21 February 2004 was associated with high back-

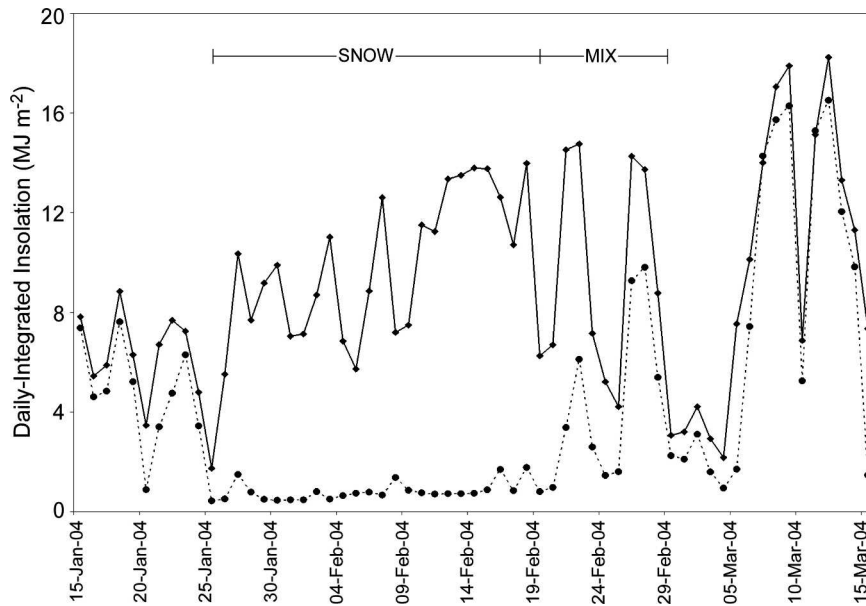


FIG. 10. Time series of daily-integrated satellite-estimated insolation (dashed line) and pyranometer insolation (solid line) for the Sioux Falls, SD, USCRN station from 15 Jan 2004 to 15 Mar 2004. Snow-covered and mixed snow-free/snow-covered conditions at the USCRN station are indicated along the top of the figure.

ground albedo and low satellite-derived insolation values. As the snowpack melted during the subsequent 2-week period, a pronounced east–west snow cover gradient developed across eastern South Dakota (Fig. 9b). This situation resulted in a mixture of snow-free and snow-covered conditions surrounding the USCRN station, which lead to improved, though still underestimated, insolation predictions. By 8 March 2004, snow-free conditions across the region resulted in much more accurate satellite estimates.

This snow cover discrimination problem will be addressed in future versions of the insolation algorithm by discarding the minimum albedo at grid cells that are identified through an independent snow mask and by assigning a representative “snow albedo” value that is based on a priori information. For example, a prototype snow albedo product has been developed for the Moderate Resolution Imaging Spectroradiometer (MODIS), yielding broadband albedos that agree with ground measurements to within 15% (Klein and Stroeve 2002). Cloud amount and cover information in this case will need to be obtained through other means, such as from operational cloud products based on GOES sounder data.

6. Conclusions

Hourly and daily integrated insolation estimates derived from GOES satellite imagery were compared to pyranometer insolation data from the USCRN for a continuous 15-month period from 1 December 2002 to 29 February 2004 (excluding days with snow cover). The results of this comprehensive survey demonstrated that the simple physical model developed by Gautier et al. (1980) and Diak and Gautier (1983) provides accurate hourly and daily integrated insolation estimates over a wide range of seasons and land surface types. The average rmsd between measurements and model predictions based on GOES-W (GOES-E) imagery was 18% (20%) and 9% (10%) of the mean observed value for hourly and daily insolation, respectively. This level of accuracy is comparable, or superior, to results from prior satellite-derived insolation studies using more complex radiative transport models. Accuracy can be improved in the overlap between GOES-E and GOES-W imaging domains by averaging insolation data independently derived from each satellite.

A detailed investigation of the insolation data at 23 USCRN stations during the fall of 2003 suggests that an elevation-related bias may exist in the physical model, resulting in a systematic underestimation of insolation for stations at higher elevations. Future improvements to the insolation model will address potential topo-

graphic biases in precipitable water/water vapor model inputs and cloud property assessments. The possible extension of model utility to include snow cover conditions will be investigated, using independent snow albedo and cloud cover information. In addition, a study is currently underway to evaluate the enhanced agreement between modeled and measured insolation data that might be achieved during inhomogeneous cloud conditions by increasing the temporal and spatial resolution of the satellite-based insolation product to 15 min and 2 km, respectively. High-resolution insolation estimates are being compared to measurements taken at a network of net radiation stations across eastern Florida, where complex cumulus cloud conditions that are associated with sea-breeze circulations and tropical convection frequently occur.

Acknowledgments. We are grateful to three anonymous reviewers, whose comments served to significantly improve this paper. This work was sponsored by the National Aeronautics and Space Administration under grants NAG1399008 and NNG04GK89G, and by the National Oceanic and Atmospheric Administration under grant NA06GP0348.

REFERENCES

- Anderson, M. C., W. L. Bland, J. M. Norman, and G. R. Diak, 2001: Canopy wetness and humidity prediction using satellite and synoptic-scale meteorological observations. *Plant Dis.*, **85**, 1018–1026.
- , W. P. Kustas, and J. M. Norman, 2003: Upscaling and downscaling—A regional view of the soil-plant-atmosphere continuum. *Agron. J.*, **95**, 1408–1432.
- , J. M. Norman, J. R. Mecikalski, R. D. Torn, W. P. Kustas, and J. B. Basara, 2004: A multiscale remote sensing model for disaggregating regional fluxes to micrometeorological scales. *J. Hydrometeorol.*, **5**, 343–363.
- Darnell, W. L., W. F. Staylor, S. K. Gupta, and F. M. Denn, 1988: Estimation of surface insolation using sun-synchronous satellite data. *J. Climate*, **1**, 820–835.
- Dedieu, G., P. Y. Deschamps, and Y. H. Kerr, 1987: Satellite estimates of solar irradiance at the surface of the earth and of surface albedo using a physical model applied to meteorosat data. *J. Climate Appl. Meteor.*, **26**, 79–87.
- Diak, G. R., and C. Gautier, 1983: Improvements to a simple physical model for estimating insolation from GOES data. *J. Climate Appl. Meteor.*, **22**, 505–508.
- , D. Kim, M. S. Whipple, and X. Wu, 1992: Preparing for the AMSU. *Bull. Amer. Meteor. Soc.*, **73**, 1971–1984.
- , W. L. Bland, and J. Mecikalski, 1996: A note on first estimates of surface insolation from GOES-8 visible satellite data. *Agric. For. Meteorol.*, **82**, 219–226.
- , M. C. Anderson, W. L. Bland, J. M. Norman, J. M. Mecikalski, and R. M. Aune, 1998: Agricultural management decisions aids driven by real-time satellite data. *Bull. Amer. Meteor. Soc.*, **79**, 1345–1355.
- Frouin, R., and B. Chertock, 1992: A technique for global moni-

- toring of net solar irradiance at the ocean surface. Part I: Model. *J. Appl. Meteor.*, **31**, 1056–1066.
- , C. Gautier, K. B. Katsaros, and R. J. Lind, 1988: A comparison of satellite and empirical formula techniques for estimating insolation over the oceans. *J. Appl. Meteor.*, **27**, 1016–1023.
- Garatuza-Payan, J., R. T. Pinker, W. J. Shuttleworth, and C. J. Watts, 2001: Solar radiation and evapotranspiration in northern Mexico estimated from remotely sensed measurements of cloudiness. *Hydrol. Sci. J.*, **46**, 465–478.
- Gautier, C., G. R. Diak, and S. Masse, 1980: A simple physical model to estimate incident solar radiation at the surface from GOES satellite data. *J. Appl. Meteor.*, **19**, 1007–1012.
- , —, and —, 1984: An investigation of the effects of spatially averaging satellite brightness measurements on the calculation of insolation. *J. Climate Appl. Meteor.*, **23**, 1380–1386.
- Higgins, R. W., Y. Yao, and X. Wang, 1997: Influence of the North American monsoon system on the United States summer precipitation regime. *J. Climate*, **10**, 2600–2622.
- Jacobs, J. M., D. A. Myers, M. C. Anderson, and G. R. Diak, 2002: GOES surface insolation to estimate wetlands evapotranspiration. *J. Hydrol.*, **56**, 53–65.
- Kawamura, H., S. Tanahashi, and T. Takahashi, 1998: Estimation of insolation over the Pacific Ocean off the Sanriku Coast. *J. Oceanogr.*, **54**, 457–468.
- Klein, A. G., and J. Stroeve, 2002: Development and validation of a snow albedo algorithm for the MODIS instrument. *Ann. Glaciol.*, **34**, 45–52.
- Lacis, A. A., and J. E. Hansen, 1974: A parameterization for absorption of solar radiation in the earth's atmosphere. *J. Atmos. Sci.*, **31**, 118–133.
- Mecikalski, J. M., G. R. Diak, M. C. Anderson, and J. M. Norman, 1999: Estimating fluxes on continental scales using remotely sensed data in an atmosphere–land exchange model. *J. Appl. Meteor.*, **38**, 1352–1369.
- Möser, W., and E. Raschke, 1984: Incident solar radiation over Europe from METEOSAT data. *J. Climate Appl. Meteor.*, **23**, 166–170.
- National Climatic Data Center, 2003: United States Climate Reference Network functional requirements document. Doc. NOAA-CRN/OSD-2003-0009R0UD0, 25 pp. [Available online at http://www1.ncdc.noaa.gov/pub/data/uscrn/documentation/program/X040_d0.pdf.]
- Paltridge, G. W., 1973: Direct measurement of water vapor absorption of solar radiation in the free atmosphere. *J. Atmos. Sci.*, **30**, 156–160.
- Pinker, R. T., and J. A. Ewing, 1985: Modeling surface solar radiation: Model formulation and validation. *J. Climate Appl. Meteor.*, **24**, 389–401.
- , and I. Laszlo, 1992: Modeling surface solar irradiance for satellite applications on global scale. *J. Appl. Meteor.*, **31**, 194–211.
- , R. Frouin, and Z. Li, 1995: A review of satellite methods to derive surface shortwave irradiance. *Remote Sens. Environ.*, **51**, 105–124.
- , and Coauthors, 2003: Surface radiation budgets in support of the GEWEX Continental-Scale International Project (GCIP) and the GEWEX Americas Prediction Project (GAPP), including the North American Land Data Assimilation System (NLDA) project. *J. Geophys. Res.*, **108**, 8798, doi:10.1029/2002JD003301.
- Raphael, C., and J. E. Hay, 1984: An assessment of models which use satellite data to estimate solar irradiance at the Earth's surface. *J. Climate Appl. Meteor.*, **23**, 832–844.
- Schmetz, J., 1989: Towards a surface radiation climatology. Retrieval of downward irradiance from satellites. *Atmos. Res.*, **23**, 287–321.
- Stewart, J. B., C. J. Watts, J. C. Rodriguez, H. A. R. De Bruin, A. R. van den Berg, and J. Garatuza-Payan, 1999: Use of satellite data to estimate radiation and evaporation for north-west Mexico. *Agric. Water Manage.*, **38**, 181–193.
- Tang, M., and E. R. Reiter, 1984: Plateau monsoons of the Northern Hemisphere: A comparison between North America and Tibet. *Mon. Wea. Rev.*, **112**, 617–637.
- Tarpley, J. D., 1979: Estimating incident solar radiation at the surface from geostationary satellite data. *J. Appl. Meteor.*, **18**, 1172–1181.
- Weymouth, G., and J. LeMarshall, 1999: An operational system to estimate global solar exposure over the Australian region from satellite observations. *Aust. Meteor. Mag.*, **48**, 181–195.